The Role of NOX2 and "Novel Oxidases" in Airway Chemoreceptor O_2 Sensing

Ernest Cutz, Jie Pan and Herman Yeger

Abstract In pulmonary neuroepithelial bodies (NEB), presumed airway chemoreceptors, classical NADPH oxidase (gp91 phox, NOX2) is co-expressed with O_2 sensitive K^+ channels (K^+O_2) and functions as an O_2 sensor. Here we examined related NADPH oxidase homologues "novel oxidases "(NOX 1, 3&4) and their possible involvement in O_2 sensing. For immunolocalization we used specific antibodies against various NADPH components and K^+ (O_2) subunits to label NEB in rat /rabbit lung and NEB related H146 tumor cell line. For gene expression profiling of NEB cells microdissected from human lung, and H146 cells, we used custom MultiGene-12TM RT-PCR array that included NADPH oxidase components and homologues /accessory proteins (NOX1-4, phox-p22, p40, p47, p67, Rac1, NOXO1 and NOXA1) and K^+O_2 channels (Kv −1.2, 1.5, 2.1, 3.1, 3.3, 3.4, 4.2, 4.3;TASK1-3). In rat lung, NOX2, NOX4, p22phox, Kv3.3 (and Kv3.4 in rabbit) and TASK1 localized to the apical plasma membrane of NEB cells, and membrane or sub-membrane regions in H146 cells. NEB and H146 cells expressed all NOX proteins except NOX3, as well as all K^+O_2 channels, except Kv1.5 and Kv4.3. Co-immunoprecipitation using Western blot multicolor Quantum dot labeling showed NOX2 molecular complexes with Kv but not with TASK, while NOX4 associated with TASK1 but not with Kv channel proteins. Hypoxia -induced serotonin release was inhibited in H 146 cells by siRNA to NOX2, while siRNA to NOX4 had only a partial effect, implicating NOX 2 as the predominant NEB cell O_2 sensor. Present findings support NEB cell specific plasma membrane model of O_2 sensing, and suggest unique NOX/K^+O_2 channel combinations for diverse physiological NEB functions.

Keywords Pulmonary neuroepithelial bodies · Oxygen sensing mechanism · Oxygen sensitive K^+channels · NADPH oxidase · Airway oxygen sensor · Hypoxia signaling

E. Cutz (✉)
Division of Pathology, Department of Pediatric Laboratory Medicine, The Research Institute, The Hospital for Sick Children and University of Toronto, Toronto, Ontario, Canada
e-mail: ernest.cutz@sickkids.ca

C. Gonzalez et al. (eds.), *Arterial Chemoreceptors*, Advances in Experimental Medicine and Biology 648, DOI 10.1007/978-90-481-2259-2_49,

1 Introduction

Pulmonary neuroepithelial bodies (NEB) form innervated clusters of amine (serotonin, 5-HT) and peptide containing cells that are widely distributed within the airway mucosa of human and animal lungs (Cutz 1997, Van Lommel et al. 1999, Linnoila 2006). NEBs are thought to function as hypoxia sensitive airway sensors involved in the control of breathing, particularly during the perinatal period (Cutz and Jackson 1999, Bolle et al. 2000).

NEB cells express a membrane delimited O_2 sensing molecular complex "O_2 sensor" composed of O_2 sensing proteins coupled to an O_2 sensitive K^+ channel (K^+ O_2) (Youngson et al. 1993, Wang et al. 1996). A potential candidate for O_2 sensing protein include the heme-linked nicotinamide adenine dinucleotide phosphate oxidase (NADPH oxidase), similar to the one identified in neutrophils (Quinn and Gauss 2004). Several lines of evidence support NADPH oxidase as the principal O_2 sensor in NEB cells including co-expression of various components of NADPH oxidase (i.e. gp91phox and p22phox) and O_2 sensitive voltage gated K^+ channel subunit $KV_{3.3a}$ (Wang et al. 1996, Cutz et al. 2003). Studies using the small cell lung carcinoma (SCLC) cell line H-146, an immortalized cell model for NEB cells, also support the role of the oxidase as an O_2 sensor (O'Kelly et al. 2000, Hartness et al. 2001, Searle et al. 2002). The definitive proof comes from studies of a mouse model with NADPH oxidase deficiency (OD; $gp91^{phox}$ k/o) (Fu et al. 2000, Kazemian et al. 2002). Taken together, the above studies provide strong evidence for the hypothesis of a membrane delimited mechanism for O_2 sensing by NEB cells which may differ from other O_2 sensing cells and may be also age dependent (Weir et al. 2005).

Other potential candidates for an O_2 sensor proteins in NEB cells include recently identified homologues of NADPH oxidase (also referred to as "low output" oxidases) that are found in a variety of non-phagocytic cells (Lambeth 2004). While the founder protein, $gp91^{phox}$ (*Nox2*) is predominantly expressed in phagocytic cells where it plays a critical role in host defense, *Nox 1* is expressed mostly in colonic epithelium, whereas *Nox 3* is expressed mainly in the fetal kidney and inner ear. *Nox 4*, originally described as a renal oxidase (Renox), is widely expressed in various tissues, including lung, placenta, pancreas, bone and blood vessels where it may be involved in various cellular processes such as cell proliferation, apoptosis and receptor signaling (Lambeth 2004). In the present study we have investigated the gene expression, localization and potential role of NOX2 and other NOX proteins as well as O_2 sensitive K^+ channels involved in O_2 sensing using the H146 tumor cell model and native NEB cells of human and animal lungs.

2 Methods

2.1 Cell Lines and Tissues

The classical SCLC cell line H146 and a lung carcinoid cell line H727 were obtained from ATCC (Manassas, VA). Control cell line included a promyelocytic cell line

(HL60, representative of neutrophils). Normal human lung tissue was obtained from a lung resection specimen from a 6 month old male infant and from human fetuses (~20 weeks gestation) obtained at autopsy, with the approval of the Human Subjects Review Committee of The Hospital for Sick Children. Lung tissues from neonatal rats and rabbits (1–5 day old) were embedded in polyethylene glycol (OCT medium)) and then snap frozen on dry ice. All animal procedures were approved by the Animal Care Committee of the Hospital for Sick Children.

2.2 Laser Capture Microdissection (LCM)

Serial frozen sections of lung (8 μm) were post- fixed in 70% ethanol at −4°C for 5 min and air-dried for 15 min at room temperature. After re-hydration in PBS, the sections were incubated in 20% normal donkey serum in 4% BSA to suppress non-specific binding. To identify NEB we used monoclonal anti-synaptic vesicle 2 (SV2) antibody (1:20 dilution; Developmental Studies Hybridoma Bank, Iowa City, IA). After incubation with biotin-conjugated secondary anti-mouse IgG antibody, streptavidin-Texas Red X conjugate was applied (Molecular Probes; Eugene, OR) for 30 min at RT. LCM was performed using the Pix-Cell II^{TM} system with CapSureTM HS LCM caps (Arcturus Engineering, Mountain View, CA) under the fluorescent microscope. Thermoplastic film containing captured cells was peeled off caps and transferred to a 0.5 ml microcentrifuge tube with 20 ml of extraction buffer (PicoPure RNA isolation kit; Arcturus Engineering). Up to 6 tubes of captured NEB and airway epithelial cells were pooled and RNA was extracted with the PicoPureTM RNA isolation kit. To obtain sufficient RNA from these cells for RT-PCR array profiling, two-round amplification procedures were performed using a RiboAmp RNA Amplification kit (Arcturus Engineering, Mountain View, CA).

2.3 Gene Expression Profiling

For cell lines, approximately 1×10^5 cells were placed in RNA lysis buffer, homogenized, and applied to RNA purification columns (SuperArray, Frederick, MD). The bound RNA was treated with DNAse I, washed and eluted. Two hundred ng of total RNA (from cell lines or from LCM/amplification samples) were processed with RT annealing mixture in custom NADPH MultiGene-12 RT PCR profiling array kit (see Table 1) and custom O_2 sensitive K^+channels MultiGene-12 RT PCR profiling array kit (see Table 2), respectively. Amplified products and DNA molecular weight markers (100 bp DNA Ladder; Invitrogen) were separated by electrophoresis in 2% agarose gels.

2.4 Immunohistochemistry

Cell lines were plated on poly-L-lysine -coated glass coverslips, fixed in Zinc-formalin solution (NewcomSupply, Middleton, WI) for 10 min at room temperature

Table 1 Nucleotide sequences of human NADPH subunits primers used for NOX MultiGene-12 RT-PCR Profiling analyses

GenBank	Symbol	Description	GeneName	Size (bp)	Ref_post (bp)
NM_000101	CYBA	Cytochrome b-245, alpha polypeptide,*p22^{phox}*	CYBA	101	381–399
NM_000397	CYBB	Cytochrome b-245, beta polypeptide,*gp91^{phox}*	CGD/GP91-1	118	1350–1368
NM_000631	NCF4	Neutrophil cytosolic factor 4, *p40^{phox}*	NCF/P40PHOX	191	1165–1185
NM_000265	NCF1	Neutrophil cytosolic factor 1, *p47^{phox}*	NOXO2/P47PHOX	97	754–772
NM_000433	NCF2	Neutrophil cytosolic factor 2, *p67^{phox}*	NOXA2/P67PHOX	101	1557–1577
NM_016931	NOX4	NADPH oxidase 4, NOX4	KOX/KOX-1	88	1643–1665
NM_015718	NOX3	NADPH oxidase 3, NOX3	GP91-3	107	1652–1672
NM_007052	NOX1	NADPH oxidase 1, NOX1	GP91-2/MOX1	88	623–645
NM_006908	RAC1	Ras-related C3 botulinum toxin substrate 1, RAC	MIG5/P21-RAC1	126	2091–2111
NM_172168	NOXO1	NADPH oxidase organizer 1, Noxo1	P41NOX/P41NOXA	82	360–378
NM_006647	NOXA1	NADPH oxidase activator 1, Noxa1	NY-CO-31/P51NOX	105	483–501
NM_002046	GAPDH	Glyceraldehyde-3-phosphate dehydrogenase	G3PD/GAPD	168	389–407

(RT), and permeabilized in 0.02% saponin in PBS with 0.1% bovine serum albumin. Cells were incubated with 4% bovine serum albumin with 10% goat serum at room temperature for 30 min. Cells were then stained at 4C overnight with anti-gp91^{phox}, anti-NOX4, anti-p22^{phox}, anti-p47^{phox} and anti-p67^{phox} polyclonal antibodies (Table 3) followed by 1 hr incubation with Texas Red-conjugated donkey anti-rabbit/goat IgG.

Cryostat sections of lung were cut at 60–80 μm and fixed in zinc formalin solution at RT. Dual immunofluorescence (*gp91^{phox}* plus SV2 antibodies/*p22^{phox}* plus SV2) labeling was performed on sections permeablized with 0.5% Triton X-100 in PBS for 10 min and incubated primary antibodies and FITC/Texas Red conjugated 2nd antibodies. For co-localization of NADPH subunits, double immunofluorescence staining was performed using goat anti-*gp91^{phox}* Nter antibody along with rabbit anti-*p22^{phox}*, *p47^{phox}* and *p67^{phox}* antibodies, respectively. Images were scanned with the multitracking mode on a Leica confocal laser scanning microscope (model TCS 4D) with SCANWARE software. The excitation wavelengths of the

Table 2 Nucleotide sequences of human K+ channel subunits primers used for potassium channel MultiGene-12 RT-PCR Profiling analyses

GenBank	Symbol	Description	GeneName	Size (bp)	Ref_post (bp)
NM_002246	KCNK3	Potassium channel, subfamily K3, TASK1	OAT1/TASK1	95	593–611
NM_003740	KCNK5	Potassium channel, subfamily K5, TASK2	TASK-2/TASK2	103	1102–1121
NM_016601	KCNK9	Potassium channel, subfamily K9. TASK3	TASK-3/TASK3	169	385–404
NM_004978	KCNC4	Potassium voltage-gated channel, shaw-subfamily4, Kv3.4	HKSHIIIC	188	737–756
NM_004980	KCND3	Potassium voltage-gated channel, Shal-subfamily3, Kv4.3	KCND3L	171	2258–2278
NM_004974	KCNA2	Potassium voltage-gated channel, shaker-subfamily2, Kv1.2	HBK5/HK4	191	736–754
NM_002234	KCNA5	Potassium voltage-gated channel, shaker-subfamily5, Kv1.5	HCK1/HK2	168	739–757
NM_004977	KCNC3	Potassium voltage-gated channel, Shaw-subfamily3, Kv3.3	KSHIIID	147	1300–1319
NM_004975	KCNB1	Potassium voltage-gated channel, Shab-subfamily1, Kv2.1	DRK1/h-DRK1	122	867–885
NM_012281	KCND2	Potassium voltage-gated channel, Shal-subfamily2, Kv4.2	RK5	118	2532–2551
NM_004976	KCNC1	Potassium voltage-gated channel, Shaw-subfamily1, Kv3.1	KV4/NGK2	142	570–590
NM_002046	GAPDH	Glyceraldehyde-3-phosphate dehydrogenase	G3PD/GAPD	168	389–407

Table 3 Primary antibodies used

Antibodies	Epitope	Host	Dilut for IF	Dilut for W/B	Sources
Anti-gp91^{phox}	Cter	rabbit	1:400	1:500	Dr Dagher
Anti-NOX4	Whol	rabbit	1:400	1:600	Dr Lambeth
Anti-gp91^{phox}	Nter	goat	1:200	1:400	Santa Cruz
Anti-p22^{phox}	Cter	rabbit	1: 500	1:500	Dr Dagher
Anti-p22^{phox}	Nter	rabiit	1:500	1:500	Dr Dagher
Anti-p47^{phox}	Cter	rabbit	1:1000	1:5000	Dr Dagher
Anti-p67^{phox}	Whol	rabbit	1:500	1:1000	Dr Dagher
Anti-Kv 1.2	Cter	goat	N/A	1:500	Santa Cruz
Anti-Kv 2.1	Cter	rabbit	N/A	1:1000	Alomone
Anti-Kv 3.4	Nter	rabbit	1:200	1:1000	Alomone
Anti-Kv 3.3	Cter	rabbit	1:400	1:1000	Alomone
Anti-Kv 4.2	Cter	goat	N/A	1:500	Santa Cruz
Anti-Kv 4.3	Nter	goat	N/A	1:1000	Santa Cruz
Anti-SV2	N/A	Mouse	1:20	N/A	Hybrydoma B

krypton/argon laser were 488 nm for FITC and 568 nm for Texas Red. Images were processed with Photoshop CS (Adobe).

2.5 Western Blotting and Co-immunoprecipitation

To obtain cell membrane proteins, H146 cells were briefly vortexed in hypotonic HEPES solution with 1X protease inhibitor cocktail and centrifuged at 800 g for 10 min at 4°C. The pellets were extracted in PBS containing 0.001% Tween 20 and 1X protease inhibitor cocktail.

For co-immunoprecipitation studies, 300 μg from each protein sample was co-precipitated with either NOX2/NOX4 or Kv channels/TASK1 antibodies using the Seize® X Protein G Immunoprecipitation kit (Pierce Inc.). For Western blots and triple-Quantum Dot (Q-dot) labeling, samples were loaded in 7% SDS-PAGE (30 ul/lane) and transferred onto a PVDF membrane. After blocking, membranes were processed through co-incubations with goat anti-NOX2, rabbit anti-Kv4.3, (or Kv3.3, Kv2.1 and Kv3.4) and mouse anti-beta-actin antibodies, and co-incubated overnight with rabbit anti-NOX4, goat anti-TASK1 and mouse anti-beta-actin antibodies, followed by incubation in Qdot® Secondary Antibody Conjugates (Qdo705 goat anti-rabbit IgG (red)/Qdot655 horse anti-goat IgG (green) and donkey anti-mouse-AMCA (blue) conjugates diluted 1:1000 in blocking buffer. ImageStation 2000 MM system with Filtered Epi Illumination (KODAK 415/100 bp) was used to capture images by CCD camera.

2.6 Plasmid Construction and Transfection of si RNA Silencing

Silencer® siRNA duplexes specific for the human *NOX2* gene (5'-GGAUACUAAC CAAUAGGA Utt -3' and 5'-AUCCUAUUGGUUAGUAUCCtt -3'), *Silencer*® siRNA duplex specific to human *NOX4* (5'-XCACCACCACCACCACCATT-3' and 5'-AAUGGUGGUGGUGGUGGU GTT-3') and a non-silencing human control duplex (directed against the target sequence, 5'-AATTCTCCGAACGTGTCACGT-3') were purchased from Ambion Inc (Applied Biosystems Canada, Streetsville, Ontario). For stable transfections with siRNA, hairpin siRNA (NOX2 and NOX4) templates were ligated and cloned in p*Silencer* 4.1-CMV neo vectors (Ambion) by a custom service from GenScript Corp (Piscataway, NJ). Propagated NOX2 and NOX4 plasmids were tranfected into $\sim 1 \times 10^5$ suspension cells in 35 mm culture dishes using LyoVec reagent (InvivoGen, San Diego, CA). Transfected cells were selected with G418 and knockdown expression levels confirmed by western blots, immunoflourescence and RT-PCR.

2.7 Hypoxia Induced 5-HT Release

To study the effects of siRNA silencing of NOX 2 and NOX 4 on hypoxia induced 5-HT release, H146 cells transfected with respective si RNAs were exposed to

hypoxia (2% O_2) for various time intervals (30 min, 1 hr, 3 hrs and 6 hrs) and the amount of 5-HT (ng/ml) released into the culture media measured using a highly sensitive ELISA assay as previously reported (Pan et al. 2002, 2006). Cells exposed to normoxia served as a negative control (baseline release) whereas cells incubated with diphenylene iodonium (DPI, 10 μM), a blocker of NADPH oxidase, was used as a positive control.

3 Results

3.1 Gene Expression Profiling of mRNA's for NOX and O_2 Sensitive K^+ Channels

In native NEB recovered by LCM, mRNA s for all NOX proteins including accessory proteins, except for NOX3 were abundantly expressed. The gene expression profile in SCLC cell lines was similar to native NEB cells except for the lack of expression of NOXA1 (an accessory protein homolog of p47) in H146 cells, while the better differentiated H727 cells showed an expression profile similar to native NEB cells (Fig. 1a). The neutrophil cell line H60, as expected, expressed mRNAs for all NOX proteins including all accessory units. On the other hand, airway epithelium obtained by LCM from the same lung samples, lacked NOX2 and NOX 3 expression respectively (Fig. 1a).

The gene expression profile of mRNAs for O_2 sensitive K^+ channels in native NEB cells included strong expression of TASK 1–3, and voltage activated K^+ channels (Kv), Kv 1.2, Kv 3.3, Kv3.4 and Kv 4.2. Expression of mRNAs for Kv 2.1 and 3.1 was realively weak and there was no signal for Kv4.3, previously demonstrated in rabbit neonatal NEB (Fu et al. 2007), suggesting possible species variation (Fig. 1b). In H146 and H727 cells, the majority of O_2 sensitive K^+ channel mRNAs were expressed, although the signal intensity varied (Fig. 1b). In control cell lines, the expression profile was variable with only some TASK or Kv mRNA's present.

3.2 Immunohistochemical Localization of NOX and K^+ Channel Epitopes

Immunohistochemical studies using H146 cells confirmed membrane and sub membrane localization of gp 91 phox/NOX2 (Fig. 2a), that co-localized with p22, and mostly cytoplasmic expression of p47 (not shown). Expression of NOX4 epitope was similar to NOX2, with predominantly membrane and sub membrane localization (Fig. 2b). In native NEB s of rat neonatal lung, NOX 2 was prominently localized in the apical cytoplasm facing the airway lumen, as would be expected of an airway sensor monitoring intraluminal O_2 concentration (Fig. 2c). The immunohistochemical localization of K^+ channel epitopes showed distinctive membrane staining of apical membrane in rabbit neonatal NEB, particularly with antibody

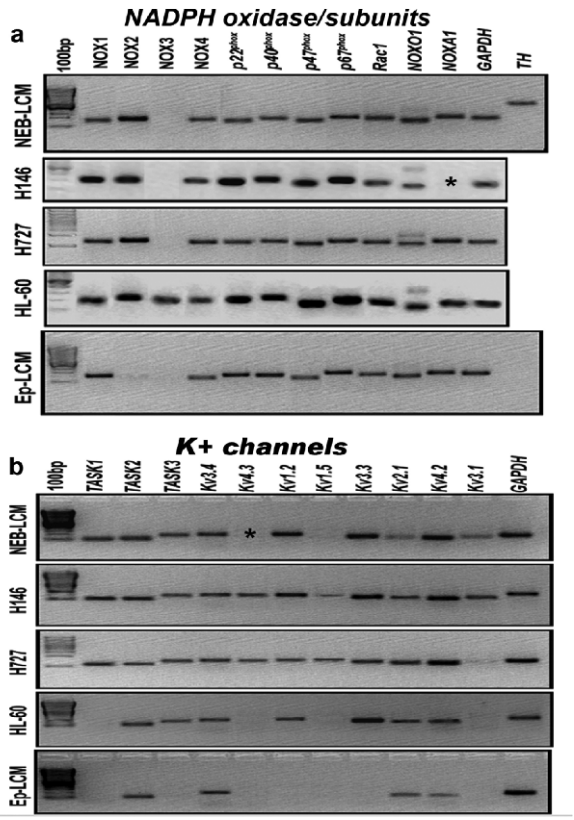

Fig. 1 Gene expression profiling for NADPH oxidase and O_2 sensitive K^+ channel mRNAs in human NEB cells obtained by laser capture micro dissection (NEB-LCM), SCLC tumor cell lines (H146, H727) and control cells (HL-60 promylocytic/neutrophil cell line; Ep-LCM airway epithelium obtained by laser capture microdissection). Note lack of expression of NOX 3 in all but HL-60 cells and no expression of NOXA1 in H146 cells

against Kv3.4 (Fig. 2d, e), and a more diffuse membrane staining with antibodies against Kv3.3 (in rat neonate) and TASK 1 in human fetal lung (not shown).

3.3 NOX/K^+ Channel Protein-Protein Interactions

To study protein-protein interactions between NOX and O_2 sensitive K^+ channels we used isolated cell membranes of H146 cells and a co-immunoprecipitation method with multicolor Quantum dot technique. In experiments with antibodies against Kv3.3/NOX2 distinct complexes of the two epitopes were obtained (Fig. 3a). In cells exposed to hypoxia (2%O_2, 6 hrs), there was significant up regulation of NOX 2 protein expression without apparent change in signal for Kv3.3 protein. On the other hand, pre-treatment of H146 cells with NOX2 siRNA significantly reduced NOX2 protein expression. Furthermore, Kv3.3/NOX2 complexes were easily dissociated with 0.005 % Triton 100, suggesting "weak" intermolecular binding. In other co-immunoprecipitation experiments we have found that while other Kv channels (i.e. Kv3.4) also formed similar complexes with NOX2, they failed to do so when NOX4 antibody was used (not shown). While TASK 1 did not form complexes with

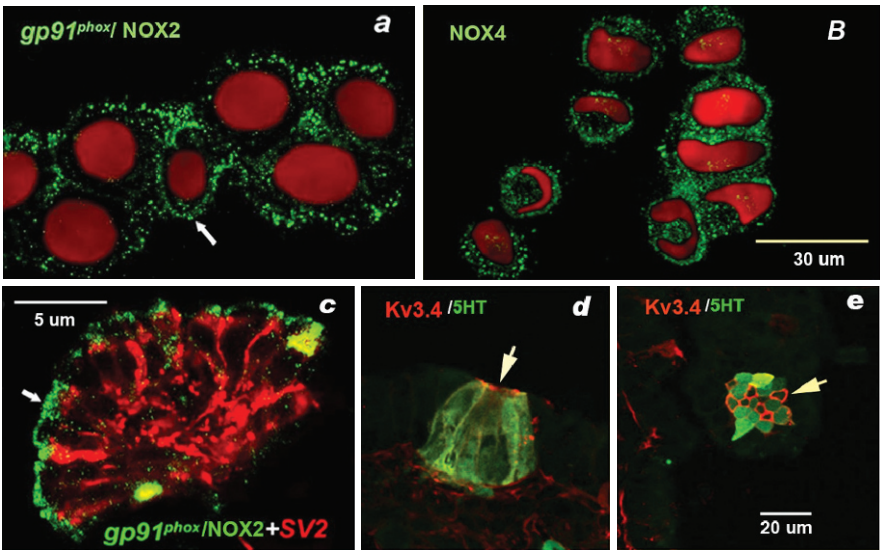

Fig. 2 Immunolocalization of NOX and Kv channel proteins in H146 and NEB cells. (**a**) Membrane and sub-membrane localization of gp91/NOX2 in H-146 cells using C-terminal directed antibody. (**b**) Localization of NOX 4 in H146 cells appears similar to NOX 2 shown in Fig. 1a. (**c**) Immunolocalization of NOX2 in NEB cells of neonatal rat lung is restricted to the apical cytoplasm facing the airway lumen (*arrow*). Double immunostaining with SV2. (**d**) Immunolocalization of Kv 3.4 subunit in NEB of neonatal rabbit lung with positive reaction confined to apical plasma membrane (*arrow*). Double immunostaining with 5-HT localized in NEB cytoplasm. (**e**) En-face view of NEB in the same sample as in Fig. 2d with distinctive linear immunostaning outlining apical cytoplasm (*arrow*)

NOX 2, it readily associated with NOX4, that was also up regulated by exposure to hypoxia (Fig. 3b).

3.4 Effects of siRNA Silencing of NOX Protein Expression on Hypoxia Induced 5-HT Secretion

Control H146 cells, maintained in normoxia showed minimal or no 5-HT release during the duration of experiments (up to 6 hrs) (Fig. 3c). The positive control cells (without siRNA silencing), showed expected time dependent hypoxia-induced 5-HT release as previously reported (Pan et al. 2002, 2006). H-146 cells transfected with NOX2 siRNA showed significant inhibition of 5-HT release after 30 min, 1 and 3 hrs exposure to hypoxia that was identical to normoxia baseline (Fig. 3c). However at 6 hrs there was an increase in 5-HT release ($p < 0.1$) above normoxia control but significantly less then the hypoxia control suggesting partial recovery of NOX2 protein expression (Fig. 3c). Using NOX4 siRNA, 5-HT release was also reduced but was less marked as compared to NOX2. Classical NADPH inhibitor, DPI (positive control) showed the expected inhibitory effect on 5-HT release.

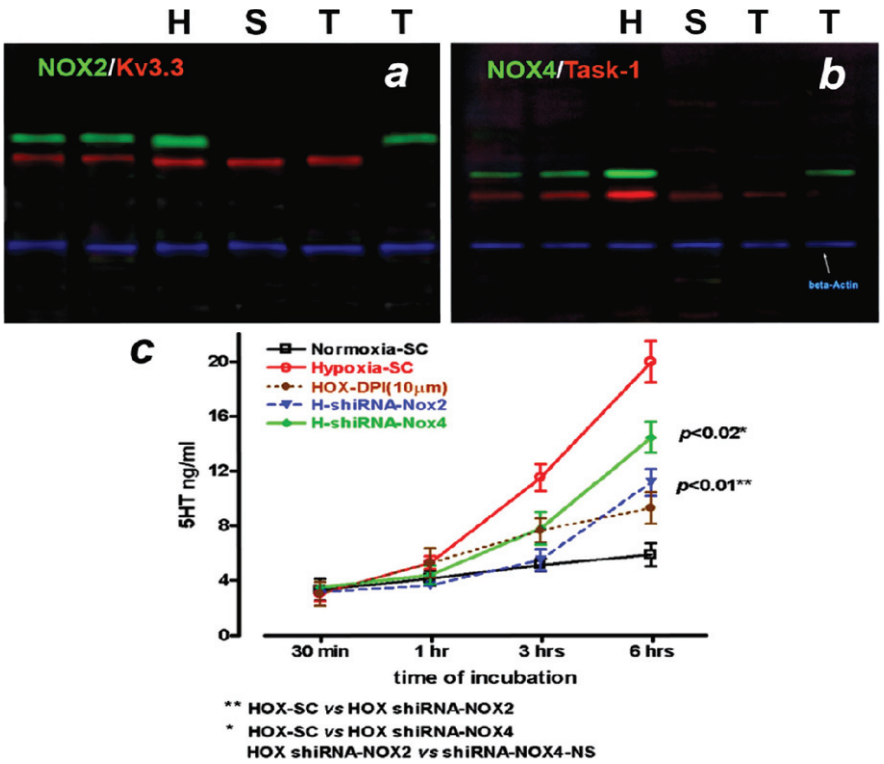

Fig. 3 (**a**) NOX2/Kv3.3 complexes in co-immunoprecipitation experiment of H146 cell membrane protein extracts using multicolor Q-dot method with antibodies against NOX 2 and KV3.3. (H) Up regulation of NOX2 protein expression after exposure to hypoxia. (S) Silencing of NOX 2 protein expression after pre-incubation with NOX2 siRNA; (T) dissociation of NOX2/Kv3.3 complexes after treatment with 0.005 Triton 100. (**b**) NOX4/TASK 1 molecular complexes using NOX4 and TASK 1 antibodies and methods as above. (H) Up regulation of NOX4 protein expression and possibly TASK1 by hypoxia and (T) dissociation of NOX4/TASK1 complexes by 0.005 Triton 100. (**c**) Effects of siRNAs for NOX2 and NOX4 on hypoxia-induced 5-HT release from H146 cells. Under normoxia (control), no significant change (baseline) over duration of experiment (6 hrs). Significant time dependent release of 5-HT in control cells exposed to hypoxia. Significant inhibition of hypoxia-induced 5-HT release after incubation with DPI (10 μM);after pre-treatment with siRNA to NOX2 after 30 min, 1 hr and 3 hrs with a partial recovery at 6 hrs. Response with siRNA for NOX4 is less marked at 3 and 6 hrs compared to NOX2

4 Discussion

The summary and conclusions of our studies reported here include: (a) Gene profiling studies revealed that both native NEB cells and related tumor cell lines express a whole range of NOX and O_2 sensitive K^+ channel proteins that comprise the membrane delimited "O_2 sensor molecular complex" (Wang et al. 1996, Cutz et al. 2003). This gene profile differs from adjacent non-endocrine airway epithelial cells. (b) Immunolocalization studies showed that "O_2 sensor molecular complex"

(NOX2/Kv3.3 etc) is localized to the plasma membrane and sub-membrane regions in representative SCLC tumor cell line (H-146), and in NEB cell apical plasma membrane as expected for an airway based sensor. (c) Co-immunoprecipitation studies showed that in H-146 cells, NOX2 but not NOX 4 forms molecular complexes with O_2 sensitive Kv channel subunits, while TASK 1 complexes with NOX4 but not with NOX2. This is in agreement with recent studies of Lee et al. (2006) showing that in HEK293 cells which endogenously express NOX 4, the activity of transfected TASK-1 channel was inhibited by hypoxia. This hypoxia response was significantly augmented by co-transfection of NOX 4, but not with NOX 2/gp91^{phox}. The O_2 sensitivity of TASK-1 was abolished by NOX 4 siRNA and NADPH inhibitors, suggesting that NOX 4 may represent the O_2 sensor protein partner for TASK-1. Taken together these observations suggest a possibility of a diversity of "O_2 sensors", even within the same cell type, matching specific NOX proteins with particular O_2 sensitive K^+ channel types (i.e. NOX 2/$KV_{3.3a}$; NOX4/TASK-1). Interestingly short term hypoxia (6 hrs) up regulated both NOX2 and NOX4 protein expression while the expression of O_2 sensitive K^+ channel proteins was unaffected. (d) Hypoxia induced 5-HT release was inhibited/reduced after siRNA silencing of NOX2 but less for NOX 4, confirming that NOX 2 is the predominant functional O_2 sensing protein in NEB related tumor cell line, and by inference in native NEB (Wang et al. 1996, Cutz et al. 2003).

Present findings support the organ and NEB specific plasma membrane model of O_2 sensing, and suggest unique NOX/K^+ channel combinations that may serve diverse NEB physiological functions in the lung.

Acknowledgments Supported by grants from Canadian Institute for Health Research, MOP-12742, MPG-15270.

References

Bolle T, Lauweryns JM, VanLommel A. 2000, Postnatal maturation of neuroepithelial bodies and carotid body innervation: a quantitative investigation in rabbit, J Neurocytol, 29:241–248.

Cutz E (Ed) 1997, Cellular and molecular biology of airway chemoreceptors. Landes bioscience, Austin, Texas.

Cutz E, Jackson A. 1999, Neuroepithelial bodies as airway chemoreceptors, Respir Physiol, 115:201–214.

Cutz E, Fu XW, Yeger H, Peers C, Kemp PJ. 2003, Oxygen sensing in Pulmonary Neuroepithelial Bodies and related tumour cell model. In Oxygen sensing: Responses and adaptation to hypoxia, eds. Lahiri S., Prabhakar H., SemenzaG., Marcel Dekker, New York, pp 567–602.

Fu XW, Wang D, Nurse CA, Dinauer MC, Cutz E. 2000, NADPH oxidase in an O_2 sensor in airway chemoreceptors: Evidence from K^+ current modulation in wild type and oxidase deficient mice, Proc Natl Acad Sci (USA), 97:4374–4379.

Fu XW, Nurse C, Cutz E. 2007, Characterization of slowly inactivating Kv alpha current in rabbit pulmonary neuroepithelial bodies:effects of hypoxia and nicotine, Am J Physiol Lung Cell Mol Physiol, 293:L892–L902.

Hartness ME, Lewis A, Searle GJ, O'Kelly I, Peers C, Kemp PJ. 2001, Combined antisense and pharmacological approaches implicate hTASK as an airway O_2 sensing K^+ channel, J Biol Chem, 276:26499–26508.

Kazemian P, Stephenson R, Yeger H, Cutz E. 2002, Respiratory control in neonatal mice with NADPH oxidase deficiency, Respir Physiol, 126:89–101.

Lambeth JD. 2004, Nox enzymes and the biology of reactive oxygen, Nature Rev Immunol 4: 181–189.

Lee YM, Kim BJ, Chun YS, So I, Choi H, Kim MS, Park JW. 2006, NOX4 as an oxygen sensor to regulate TASK-1 activity, Cellular Signalling, 18 :499–507.

Linnoila RI. 2006, Functional facets of the pulmonary neuroendocrine system, Lab Invest, 86: 425–444.

O'Kelly I, Lewis A, Peers C, Kemp PJ. 2000, O_2 sensing in airway chemoreceptor- derived cells: protein kinase C activation reveals functional evidence for involvement of NADPH oxidase, J Biol Chem, 275:7684–7692.

Pan J, Bear C, Farragher S, Cutz E, Yeger H. 2002, CFTR modulates neurosecretory function in pulmonary neuroendocrine cell related tumor cell line, Am J Resp Cell Mol Biol, 27:553–560.

Pan J, Copland I, Post M, Yeger H, Cutz E. 2006, Mechanical stretch-induced serotonin release from pulmonary neuroendocrine cells :implications for lung development, Am J Physiol Lung Cell Mol Physiol, 290:L185–L193.

Quinn MT, Gauss KA. Structure and regulation of neutrophil respiratory burst oxidase: comparison with physiological oxidases. J Leukocyte Biol 2004;76: 760–81.

Searle GJ, Hartness ME, Peers C, Kemp PJ. 2002, Lack of contribution of mitochondrial electron transport to acute O_2 sensing in model airway chemoreceptors, Biochem Biophys Res Commun, 291: 332–337.

Van Lommel A, Bolle T, Fannes W, Lauweryns JM. 1999, The pulmonary neuroendocrine system:the past decade, Arch Histol Cytol, 62:1–16.

Wang D, Youngson C, Wong V, Yeger H, Dinauer MC, Vega-Saenz de Meira E, Rudy B and Cutz E. 1996, NADPH oxidase and hydrogen peroxide-sensitive K^+ channel may function as an oxygen sensor complex in airway chemoreceptors and small cell carcinoma cell lines Proc Natl Acad Sci (USA), 93:13182–87.

Weir EK, Lopez Barneo J, Buckler KJ, Archer SL. 2005, Acute oxygen sensing mechanisms, New Engl J Med 353::2042–2055.

Youngson C, Nurse C, Yeger H, Cutz E. 1993, Oxygen sensing in airway chemoreceptors, Nature (London), 365: 153–156.